Earthq Eng & Eng Vib (2010) 9: 523-532 **DOI**: 10.1007/s11803-010-0034-0

Experimental study on interaction between membrane structures and wind environment

Yang Qingshan[1†], Wu Yue[2†] and Zhu Weiliang[1‡]

1. *School of Civil Engineering, Beijing Jiaotong University, Beijing 100044, China*

2. *School of Civil Engineering, Harbin Institute of Technology, Harbin 150006, China*

Abstract: The interaction between membrane structures and their environment can be either static or dynamic. Static interaction refers to interaction with static air, while dynamic interaction refers to wind and its effects. They can be evaluated by two parameters, added mass and radiation /aerodynamic damping, which are experimentally investigated in this study. The study includes the effects of both the static and dynamic interaction on structural dynamic characteristics, and the relationship between the interaction parameters and the covered area of a membrane structure for the static interaction and the relationship between the interaction parameters and wind direction and speed for the dynamic interaction. Experimental data show that the dynamic interaction is strongly correlated with the structural modes, i.e., the interaction of the symmetric modes is much larger than the anti-symmetric modes; and the influence of the dynamic interaction is significant in wind-induced response analysis and cannot be ignored. In addition, it is concluded that the structural natural frequency is remarkably decreased by this interaction, and the frequency band is significantly broadened.

Keywords: membrane structure; structure-air/wind interaction; added mass; aerodynamic damping; aero-elastic model

1 Introduction

Membrane structures with light weight and low stiffness often experience large displacement, velocity and acceleration under wind load, and the pattern of air-flow around the structure may be modified significantly. The result is that the interaction between the wind and the structure should be considered in the analysis of the wind-induced response of membrane structures.

Yang *et al.* (2003) grouped this interaction as static and dynamic. The former refers to the interaction between the vibrating membrane and the static air; while the latter refers to the interaction between the wind-induced vibrating structure and the wind. Static interaction may be viewed as a simple and special case of dynamic interaction. Both types can be modeled as:

$$(M_{\mathrm{S}} + M_{\mathrm{a}})\ddot{x}(t) + (C_{\mathrm{S}} + C_{\mathrm{ae}})\dot{x}(t) + \left(K_{\mathrm{S}} + K_{\mathrm{as}}\right)x(t) = p(t) \tag{1}$$

where $x(t)$, $\dot{x}(t)$, $\ddot{x}(t)$ are the structural displacement, velocity and acceleration, respectively; M_{S}, C_{S}, K_{S} are the mass, damping and stiffness of the structure, respectively; M_{a} is the added mass, which is the air mass effected by structural vibration; C_{ae} represents the aerodynamic damping for the dynamic interaction, or the radiation damping for the static interaction, which reflects the obstacle effect of the static air to the vibrating structures; K_{as} is the aerodynamic stiffness, which can be recognized as the difference between the indoor and outdoor pressures; and $p(t)$ is the exciting force.

Aerodynamic parameters have been studied by many researchers; however, much additional work is still needed to better understand this phenomena. Elashkar and Novak (1983) reviewed similarity requirements and investigated its role in free- and wind-induced vibration. Kawamura and Kiuchi (1986), Takeda *et al.* (1986), and Ishii (1997) carried out some model tests on the free vibration characteristics of cable-membrane structures. Daw and Davenport (1989) tested a forced flexible semi-cylindrical shell model in a wind tunnel and concluded that the aerodynamic coefficients are dependent upon the shape of a structure and are related to amplitude. The free vibration of large-span, self-supported, lightweight roofs backed by cavities with wall openings was experimentally investigated by Novak and Kassem (1990). He researched the influence of the wall openings on frequency and the total damping of the structure and compared it with a theory they proposed. The results showed that the air movement through the wall openings as well as the acoustical damping associated with the motion of both the roof and the air mass at the openings has a significant effect on the roof natural frequencies

Correspondence to: Yang Qingshan, School of Civil Engineering, Beijing Jiaotong University, Beijing 100044, China
Tel: +86-10-5168-8285; Fax: +86-10-5168-7250
E-mail: qshyang@bjtu.edu.cn
†Professor; ‡PhD

Supported by: National Natural Science Foundation of China Under Grant No. 50725826, 90815021
Received November 5, 2009; **Accepted** July 30, 2010

and modal damping. Il'chenko and Temnenko (1993) studied the free oscillations of a piece of membrane that is orthogonal to an inflowing stream, where a numerical hydrodynamic scheme was applied to analyze the structural response and the influence of aerodynamic damping. Kawai *et al*. (1999) discussed the flutter-like vibrations of a cantilevered roof based on an aero-elastic wind tunnel test. It was shown that the vibrations occurred from a particular wind velocity due to the lowered natural frequency, which was induced by the positive aerodynamic stiffness and the vortex-excited negative damping. Yang *et al*. (2003), Wang and Yang (2003) and Wang *et al*. (2003) provided theoretical equations for calculating the added mass and aerodynamic damping based on the simplified potential fluid theory. Yang and Liu (2005) established an analytical equation for the critical wind speed of the wind-induced instability, which can consider the effect of negative aerodynamic damping by combining the non-moment theory of thin shells and the potential fluid theory.

Further experimental and theoretical studies are necessary since the test cases are very limited and current theoretical knowledge is not systematic enough to form the basis for solid conclusions. Based on some preliminary results reported by the authors (Yang *et al*., 2008; Wu *et al*., 2008), the added mass and the radiation/aerodynamic damping are further studied experimentally in this paper. As these interaction parameters are always coupled with the structural mass and damping during an interaction process, it is necessary to find out how to separate them from the coupled mass and damping. A method to separate the added mass and the aerodynamic damping from the coupled mass and damping is introduced in detail, results are provided, and their influence on the dynamic characteristics and the responses are discussed.

2 Experimental study on static interaction

2.1 Methodology

A structure and the surrounding air become a coupled system when the air around it moves together with the vibrating structure. The total mass M_T and total damping ratio ξ_T of the vibrating system can be written as:

$$M_T = M_S + M_a \tag{2a}$$

$$\xi_T = \xi_S + \xi_{ae} \tag{2b}$$

where ξ_S, ξ_{ae} are the desired structural and radiation damping ratios, respectively.

The structure mass M_S , the total damping ratio ξ_T, and the structure and (or) the system frequencies can be measured by the experimental tests. The desired parameters M_a and ξ_{ae} may be obtained from these measured parameters, as the relationship between the mass and vibration frequency of a single degree of freedom (SDOF) system can be written as:

$$\omega_S^2 = K_S / M_S \tag{3a}$$

$$\omega_T^2 = K_T / M_T \tag{3b}$$

where ω_S, ω_T are the structural circular frequencies, and K_S, K_T are the structural stiffness without and with interaction, respectively.

It is reasonable to assume that the structural stiffness remains constant for an opening structure, i.e., K_S=K_T, and then the ratio of added mass M_a to structural mass M_S can be obtained from Eqs. (3a) and (3b):

$$M_a / M_S = (\omega_S / \omega_T)^2 - 1 \tag{4}$$

consequently, the added mass M_a can be obtained from Eq. (4) once ω_S, ω_T (i.e., the structural frequencies, $f_S = \omega_S / 2\pi$, $f_T = \omega_T / 2\pi$) and M_S are measured.

The damping ratio may be defined by the Half-PSD (power spectral density) method, i.e., there is a relationship between the damping ratio and the width of the frequency band $\Delta\omega$ that corresponds to the half-peak-value of the power spectrum (Seybert, 1981):

$$\xi = \frac{\Delta f}{2 f_0} \tag{5}$$

where f_0 is the frequency corresponding to the peak value of the power spectrum. If both the structural damping ratio and the system damping ratio can be obtained from Eq. (5), the radiation damping ratio can be obtained from $\xi_{ae} = \xi_T - \xi_S$.

Since the interaction between the structure and the air always exists during its vibrating process, a primary objective is to obtain the frequency and damping without this interaction. The methodology used in this test is as follows:

(1) According to the mechanics equivalent principle, the membrane structure is decomposed into a cable net structure and its covered membrane. The former is used to absorb the tensile force and offers the structure mass and stiffness; the latter is used as the cladding material as an obstacle to the air.

(2) The cable net structure, without the covered membrane, is made to vibrate freely in the static atmosphere by setting an initial displacement, and then the time histories of the displacement and the acceleration are recorded.

In this case, the interaction between the cable net structure (without cladding material) and the surrounding air is weak enough to be ignored. The structural frequency f_S can be obtained by applying FFT to the recorded time history, and the damping ratio ξ_S can be obtained from the power spectrum density of the recorded acceleration time history by directly applying Eq. (5).

(3) The cable net structure with a covered membrane (while the membrane mass itself is very small and has a negligible influence on the structural mass and damping)

are made to vibrate freely in the static atmosphere by setting an initial displacement, and then recording the time histories of the displacement and the acceleration.

In this case, the system frequency with interaction f_T and the damping ratio with interaction ξ_T can be obtained by following the same procedures shown in step 2. Then, the radiation damping ratio is obtained by $\xi_{ae} = \xi_T - \xi_S$ and the added mass can be deduced from Eq. 4 by the measured f_S, f_T and M_S.

2.2 Experimental model and test cases

Two classical rhombic-planed membrane structures with different sags were modeled and tested. The geometric scale ratio is 1:50; the diagonal length of the model is 60 cm, as shown in Fig. 1. The sag-diagonal ratio is *d/L*=1/12 for M-1 and *d/L*=1/8 for M-2. Based on the dynamic similarity principles, the pre-tension force is determined to be 3.8 N/cable and 4.2 N/cable for the cable net models (M-1 and M-2), and 0.5 N/cm for the membrane models (M-3 and M-4), respectively, to make their frequencies equal to the prototypes. The structural mass of all the models is 120 g, in which 100 g is offered by the steel cables and 20 g is offered by the silk membrane.

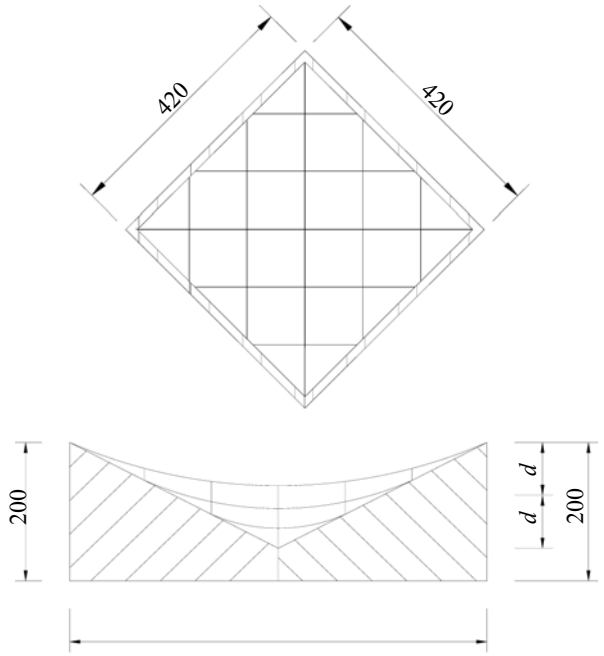

Fig. 1 Model sketch

To specify the layout of the measurement points, the test model was analyzed by FEM in advance, and the first six modes vibrate globally, as presented in Fig. 2. Modes 1 and 3 are symmetric and modes 2, 4, 5 and 6 are anti-symmetric. It is found that Modes of the membrane structure distribute closely, as indicated by Qin (2008). FEM analysis also showed that higher modes vibrate locally, but this phenomena is not discussed further in this paper.

The measured points were selected to enable all the vibration modes to be excited and recorded, as shown in Fig. 3. An initial displacement was applied to Point 3 to excite the symmetric modes, and to Points 2 and 4 (or 1 and 5) to excite the anti-symmetric modes, respectively. The acceleration sensor weighed 0.5 g and a non-contact laser displacement sensor was applied, as shown in Fig. 4. The recording frequency is 100 Hz.

The covered membrane was divided into sections and loosely attached to the joints of the cable net to avoid adding stiffness to the structure. Six cases with different covered areas for M-1(Fig. 5) were studied, where Cases 1, 4, 5, 6 are used to study the influence of the covered area on the structural dynamic characteristics; while Cases 2 and 3 are used to check whether the attached covered material offers additional stiffness to the structure. Four cases (Fig. 6) were tested for M-2 as well. As the mass of the covered membrane is very light, it is believed that it is the same for each of the different cases, and is denoted as the structural mass, i.e., the sum of the cable and the membrane as their nominated mass.

2.3 Experimental results

2.3.1 Validity checking

The recorded accelerations were analyzed by FFT and PSD functions for Cases 1 and 3 of M-1 and are shown in Fig. 7.

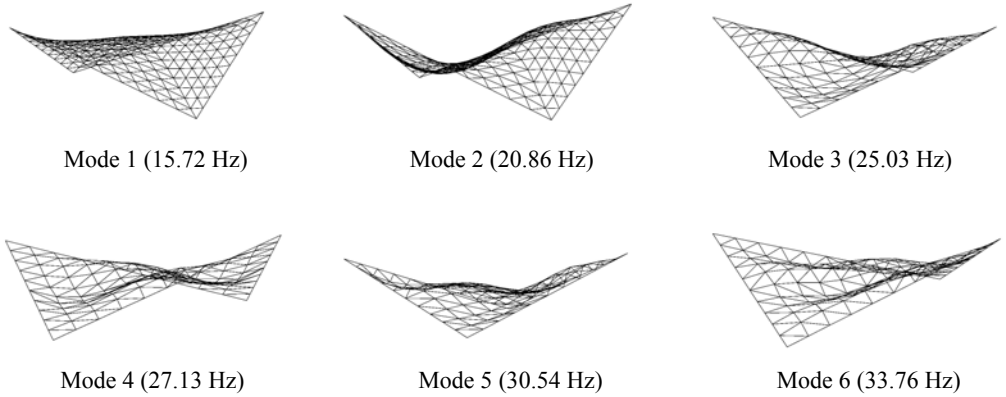

Fig. 2 First six FEM modes of Model 1

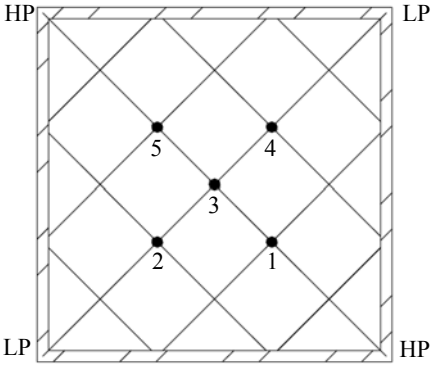

Fig. 3 Layout of measured points

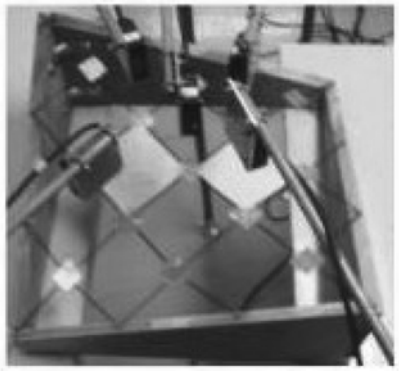

Fig. 4 Tested model

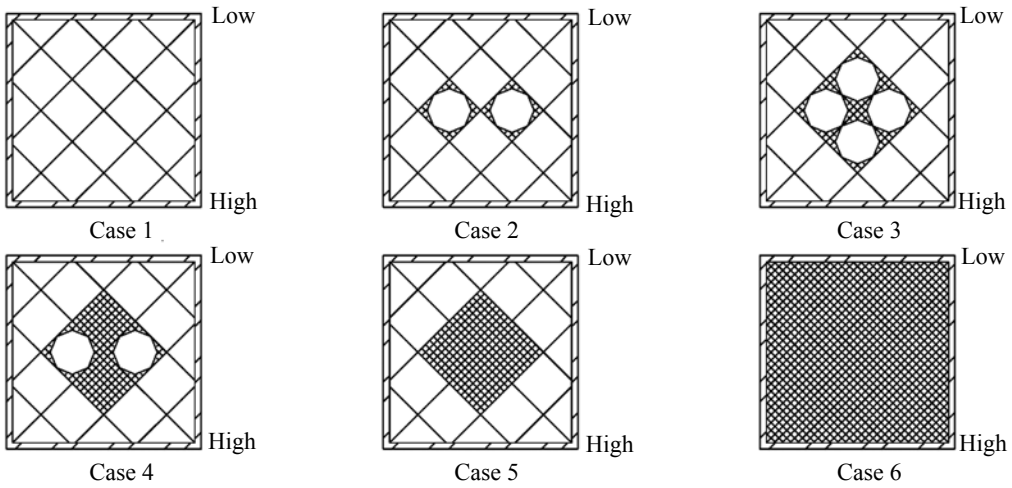

Fig. 5 Load cases for M-1 (Case 1: No cover; Case 2: 2-hole; Case 3: 4-hole; Case 4: 11% covered; Case 5: 22% covered; Case 6:100% covered

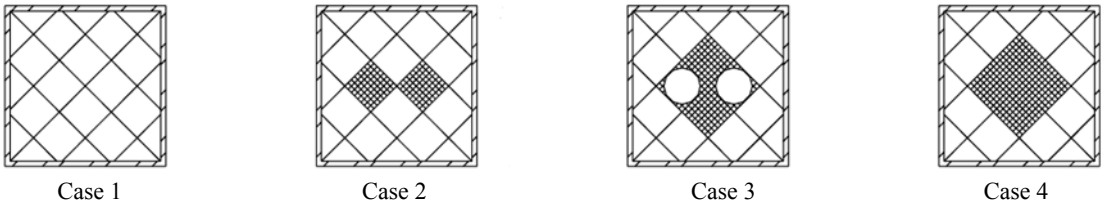

Fig. 6 Load cases of M-2 (Case 1: No cover; Case 2: 11% covered; Case 3: 11% covered and holed; Case 4: 22% covered)

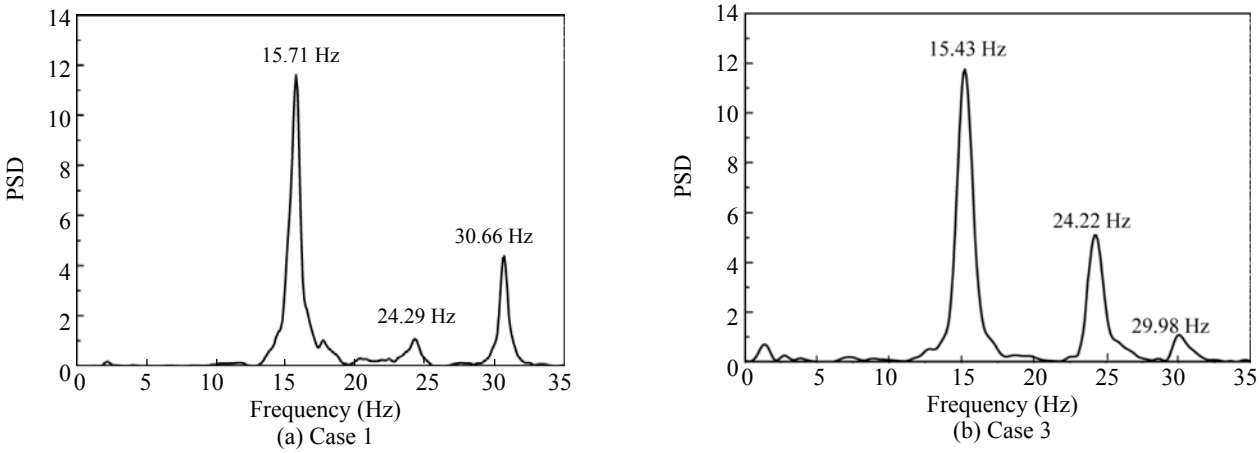

Fig. 7 Acceleration PSD at Point 4 of M-1 to determine the influence of covered material

Compared to Fig. 2, it is found that only Modes 1, 3 and 6 are recognized. As modes of the membrane structures are closely distributed (Qin, 2008), it is difficult to recognize all the modes in a test. Note that the methodology in this section is valid no matter which mode is recognized. For the recognized modes, some additional details about the natural frequencies and damping ratios of Cases 1, 2 and 3 of M-1 are listed in Table 1 to determine the influence of the attached cover. Note that the frequencies and damping ratios in these cases are almost the same, i.e., the loose cladding material does not offer additional stiffness to the structure.

Similar tests and analysis were carried out for Model M-2 and similar conclusions to those of M-1 were obtained. Table 2 lists some of the results. The small change in the frequency magnitude and band width illustrates again that the cover material does not contribute any additional stiffness to the structure.

Therefore, this suggests that the structural stiffness is mainly supplied by "cable-net," while the cover material simply sustains the air effect. In other words, the assumption $K_S = K_T$ is correct, which guarantees that the analysis in the following section is reasonable.

2.3.2 Structural dynamic behaviors

Following the procedures given in Section 2.1, the dynamic characteristics of the cable nets with different covered areas for M-1 and M-2 were analyzed. The acceleration power spectra at Point 4 of M-1 with different covered areas is shown in Fig. 8, as a representative example.

Table 1 Influence of covered material on vibration characteristics of M-1

Cases	Excited pattern*	Mode 1		Mode 3		Mode 6	
		Frequency (Hz)	Damping ratio (%)	Frequency (Hz)	Damping ratio (%)	Frequency (Hz)	Damping ratio (%)
1	a	15.67	3.22	24.58	1.65	33.69	1.18
	b	15.69	3.25	24.34	1.95	30.31	1.92
2	a	15.51	4.20	24.20	2.53	30.10	2.18
	b	15.60	4.89	24.28	2.59	30.24	2.03
3	a	15.43	5.30	24.22	1.89	29.98	2.12
	b	15.46	5.91	24.12	2.31	29.95	2.22

*Note:** Pattern a shows that Point 3 in Fig. 3 is excited; and Pattern b shows that Points 1 and 4 (or 2 and 5) are excited synchronically. This note also applies to the related tables below

Table 2 Influence of cover material on vibration characteristics of M-2

Cases	Excited pattern	Mode 1		Mode 3		Mode 6	
		Frequency (Hz)	Damping ratio (%)	Frequency (Hz)	Damping ratio (%)	Frequency (Hz)	Damping ratio (%)
1	a	15.63	0.64	25.1	0.41	31.25	0.52
	b	15.63	0.68	25.2	0.41	31.25	0.46
2	a	14.75	8.42	24.93	2.22	31.97	2.07
	b	14.55	7.58	24.96	2.55	31.33	1.72
3	a	14.55	7.53	25.0	3.73	31.70	1.94
	b	14.55	8.17	24.73	2.31	30.92	1.82

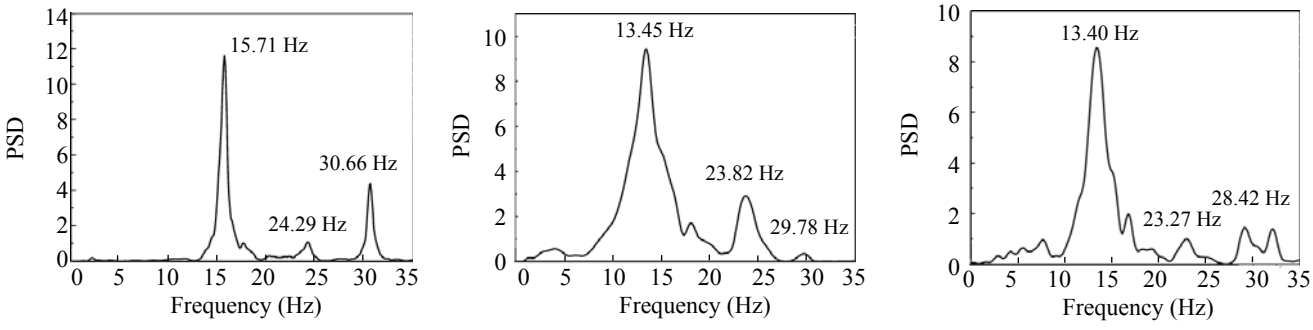

(a) Case 1 (b) Case 5 (c) Case 6

Fig. 8 Acceleration power spectrum at point 4 on M-1 with different covered cladding

It is seen from the results of the analysis that the natural frequencies of the structure without covered cladding distribute separately (i.e., the interaction can be ignored); the covered cladding decreases the natural frequencies of the structure and broadens the spectral band, i.e., more vibration modes were excited. It can be inferred that the vibration frequencies of the actual membrane structures are low and continuously distribute in a wide band.

2.3.3 Interaction parameters

(a) Added mass

The calculated ratios of the frequency with a covered membrane (i.e., including the interaction) to that without a covered membrane, f_T / f_S, are presented in Figs. 9 and 10. It is shown that the first natural frequencies of the structure decrease as the covered area increases, up to 15%.

The ratio of the added mass to the structural mass for the different covered areas and different modes can be obtained from Eq. (4) and the results for the first mode are listed in Table 3. Note that the ratio of the added mass to the structural mass is up to 37.10% for the full covered case. By the way, it is also shown that the increasing rate of the added mass becomes small when the ratio of the covered area goes beyond 22%. This is because the increased cover area from Case 5 to Case 6, which is located on the border of the structure with small movement, cannot excite the surrounding air.

Comparatively, the decrease in the 3rd and 6th frequencies is much less than the decrease in the 1st frequency. This is because the movement of each point in the first mode is in the same direction, and can excite more surrounding air; while the movement of one half area in Modes 1 and 6 is out of phase with the other half, resulting in less surrounding air becoming excited.

(b) Radiation damping

The damping ratios for these three modes, obtained from Eq. (5) and the PSD, are illustrated in Figs. 11 and 12 for M-1 and M-2, respectively.

Figure 11 shows the damping ratio of the 1st mode of Case 1, i.e., the cable net without covered membrane, is about 3%, and the damping ratio increases as the covered membrane significantly increases. It can reach up to 12% when the coverage ratio is up to 22%, and the corresponding radiation damping ratio $\xi_{ae} = \xi_T - \xi_S$ is 9%. The first mode of the damping ratio for the full covered case is 10%, less than that of the case with a 22% area covered, which may have been induced by test errors or other unknown reasons. In any case, the radiation damping ratio is much larger than the structural damping ratio. A similar conclusion can be obtained from the results for M-2, shown in Fig. 12.

Compared with the damping ratio of the 1st mode, the increase of the 3rd and 6th mode damping ratios is much less, which is similar to the case of the added masses.

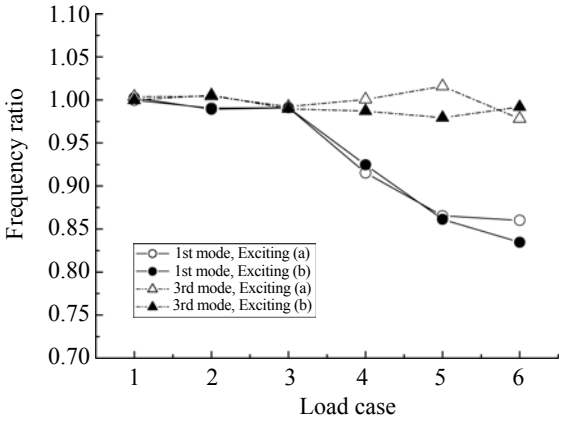

Fig. 9 Frequency ratio of M-1

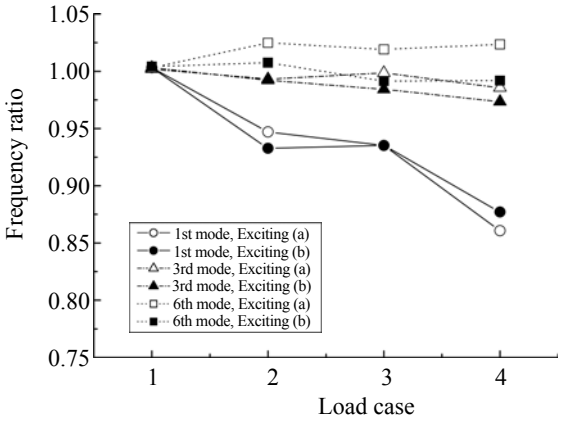

Fig. 10 Frequency ratio of M-2

Table 3 Ratio of added mass to structural mass of M-1 and M-2 (M_a/M_S) with different coverage ratio

		Coverage ratio (%)			
Model	Exciting	0	11	22	100
M-1	a	0	20.42	35.13	35.74
	b	0	17.90	36.08	37.10
		Coverage ratio (%)			
Model	Exciting	0	11	22	
M-2	a	0	12.88	35.65	
	b	0	15.40	31.12	

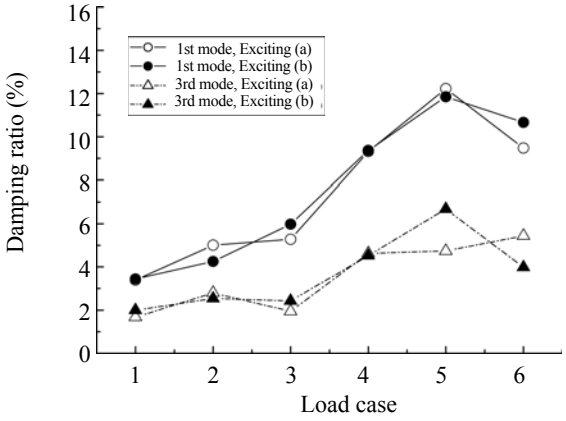

Fig. 11 Damping ratio vs load case for M-1

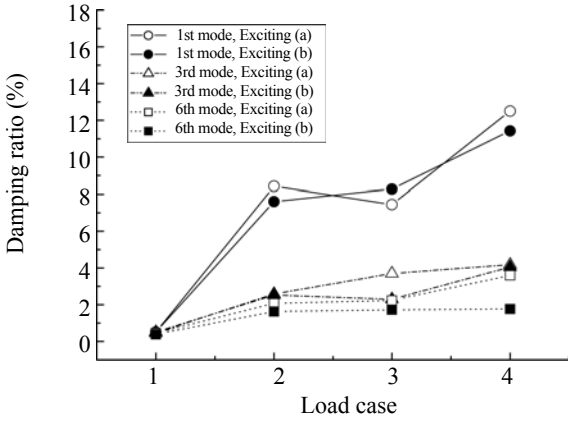

Fig. 12 Damping ratio vs load case for M-2

3 Experimental study on dynamic interaction

The dynamic interaction was tested in a wind tunnel, where the structural responses such as displacement and acceleration were recorded and then de-composed into harmonic components with different frequencies. It is believed that in the Random Decrement Technique (RDT, Ibrahim, 1977), the harmonic response components are the free vibration of an SDOF system that corresponds to different structural modes under different initial conditions, and the aerodynamic damping and added mass can be obtained from these harmonic responses.

3.1 Model test

The test was carried out in a boundary layer wind tunnel at Tongji University. The wind tunnel is of the re-circulating type with a working section 3 m×2.5 m and 12 m length over which the boundary layer is developed. Turbulent boundary layers were generated on the wind tunnel floor by using a set of vortice generators together with a carpet and a number of small cubes distributed on the floor. The mean velocity profile and turbulence intensity profile for the simulation are shown in Fig.13, with the target values for a suburban terrain category of $\alpha = 0.16$.

M-3 and M-4 (Fig. 14), two aero-elastic models of membrane structures with a prestress of 0.5 N/cm and the same dimensional size as M-1 and M-2, were designed to satisfy the similarity laws. Nine acceleration sensors were attached to each model (Fig. 15).

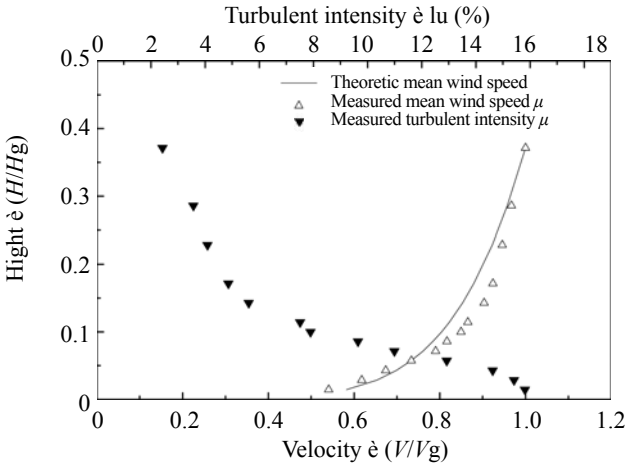

Fig. 13 Comparisons of wind tunnel simulation for terrain

Fig. 14 Aero-elastic model for wind tunnel test

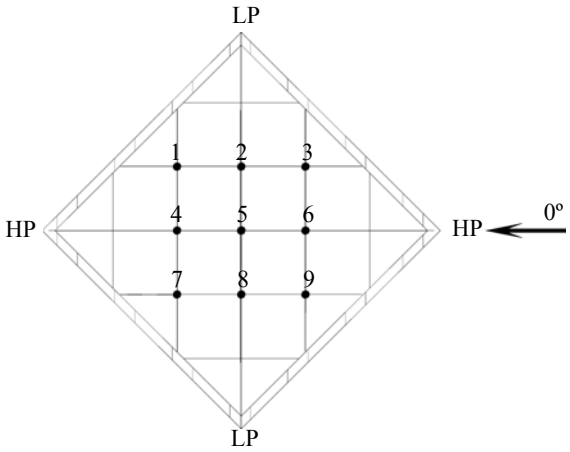

Fig. 15 Layout of acceleration sensors

3.2 Results and analysis

The response of these models for different velocities (3 m/s, 6 m/s, 9 m/s, 12 m/s, 15 m/s) and different wind directions (0°, 45°, 90°) were recorded. The Random Decrement Technique was applied to the recorded responses and three free vibration responses were obtained for each record. Some representative results are presented in the following subsections.

3.2.1 Aerodynamic damping

The free vibration responses at Point 5 on M-3 for a wind speed of 3 m/s and an angle of attack of 0 are shown in Fig. 16. Note that the recognized modes with the dynamic interaction (denoted as Mode 1, 2 and 3) are not the same as those with only the static interaction, and the damping for Modes 1 and 2 is larger than for Mode 3, as the vibration response of the first two modes decays more rapidly.

The damping ratios for Mode 1, 2, and 3 for different wind speeds and angles of attack are shown in Fig. 16.

Figure 17 shows that the 1st damping ratio of the coupling system is the largest, which can be up to 20% – 30% (including structural and radiation damping, 12% for Mode 1, measured in advance); the damping ratio for mode 2 is about 15%; and the damping ratio for Mode 3 is around 7%. The damping ratios for Modes 1 and 2 fluctuate as the wind speed changes; while the damping ratio for Mode 3 has a smaller fluctuation, which is believed to be because the membrane surface experiences suction force during the test and the correlation between the wind load and Mode 1 is stronger than that of Modes 2 and 3.

It is found that some free vibration responses increase with time and have a tendency to be divergent in a short period (Fig. 18). These types of records occur at Points 3, 7 and 8, excited by wind with speeds of 9 m/s and 12 m/s. This phenomenon may be attributed to the negative aerodynamic damping, indicating that the dynamic interaction may induce unstable flutter-like vibration as observed by Kawai *et al*. (1999).

3.2.2 Added mass

The added mass in dynamic interaction can also be obtained from Eq. (4) after the free vibration responses have been obtained, as the natural frequency without interaction was measured in Section 2. The analysis results (Fig. 19) show that the ratio of the added mass to the structural mass fluctuates from 1.2 to 0.2 as the wind speed increased from 3 m/s to 15 m/s, which implies that the correlation between the wind load and the vibration acceleration becomes weaker as the wind speed increases.

The added mass in dynamic interaction is usually almost in the same order of the structure mass, and much larger than in static interaction. However, this result is quite different from some other predictions that state that the added mass may reach about 10 times the structural mass (Daw and Davenport, 1989; Ohkuma and Marukawa, 1989). The difference indicates that the interaction between the wind and the flexible structures is very complicated and further studies are needed.

4 Concluding remarks

Based on the experimental test results, the interaction between the membrane structure and the wind environment is proven to exist, and some quantitative results can be summarized as follows:

Static interaction

(1) The added mass and the radiation damping are proven to exist according to the measured modal frequency with different covered areas, and the interaction significantly influences the structural natural frequencies. The power spectrum of the structural responses is distributed in a wide-band scope.

(2) The structural natural frequency decreases greatly, up to 15%, due to the effects of the added mass. The added mass can reach 37% of the structure mass, and the radiation damping ratio can be up to 9%.

(3) The static interaction between the membrane structures and the air is strongly relevant to the movement of the point of concern relative to its surrounding air. The interaction of the in-phase mode is much stronger.

Dynamic interaction

(1) The damping ratio for the system including interaction is much larger than the structural damping. The damping ratio for Mode 1 is 25%, larger than for Modes 2 and 3, 15% and 7%, respectively. The aerodynamic damping is influenced by the wind speed and the relevance of structural vibration to wind loading.

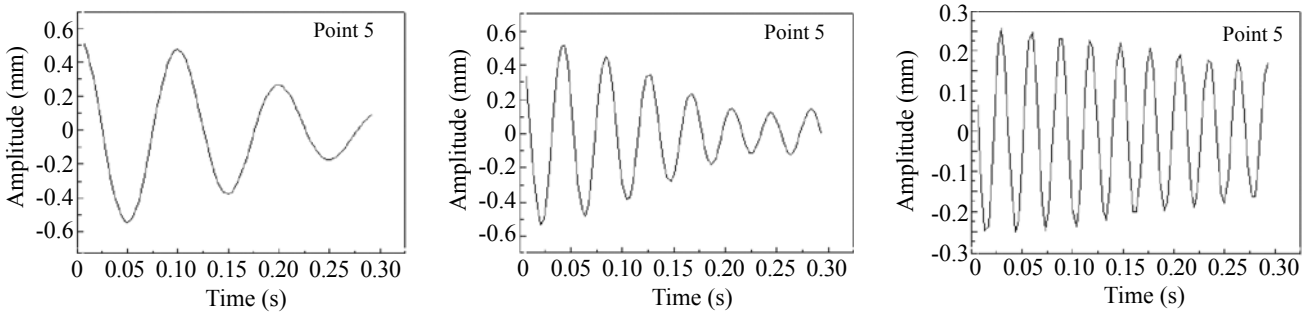

(a) f_1 = 10.11 Hz (b) f_2 = 23.60 Hz (c) f_3 = 33.71 Hz

Fig. 16 Free vibration responses of Modes 1, 2 and 3

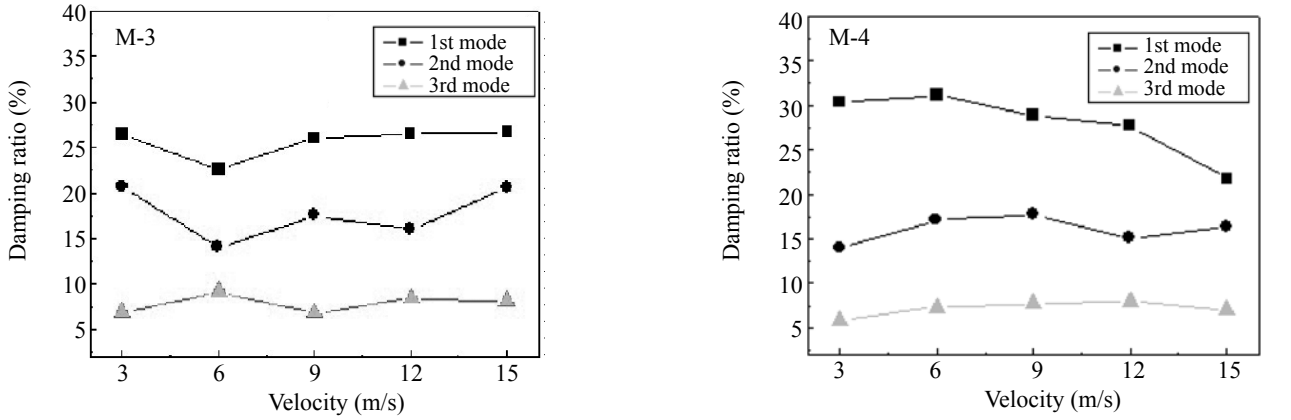

(a) 0º angle of attack

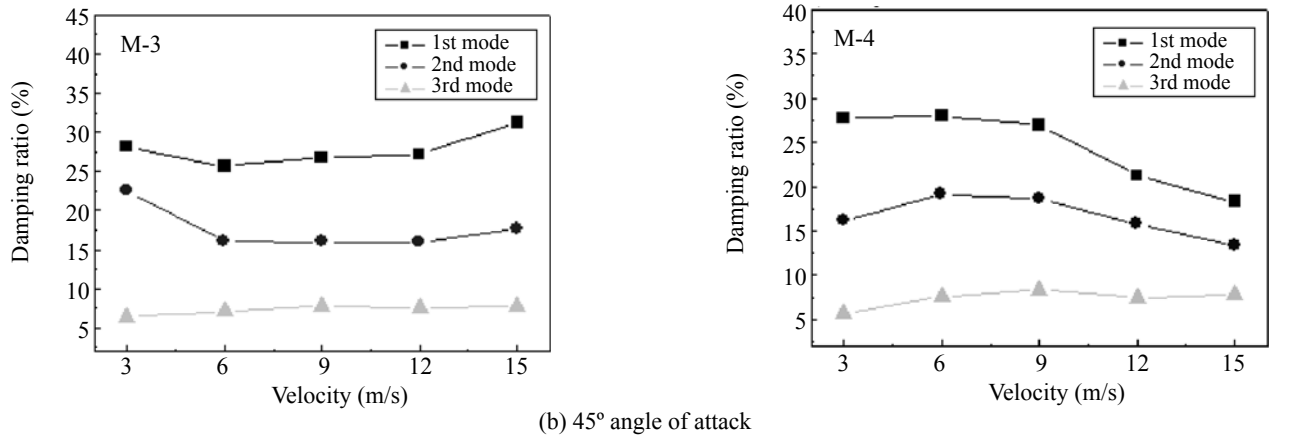

(b) 45º angle of attack

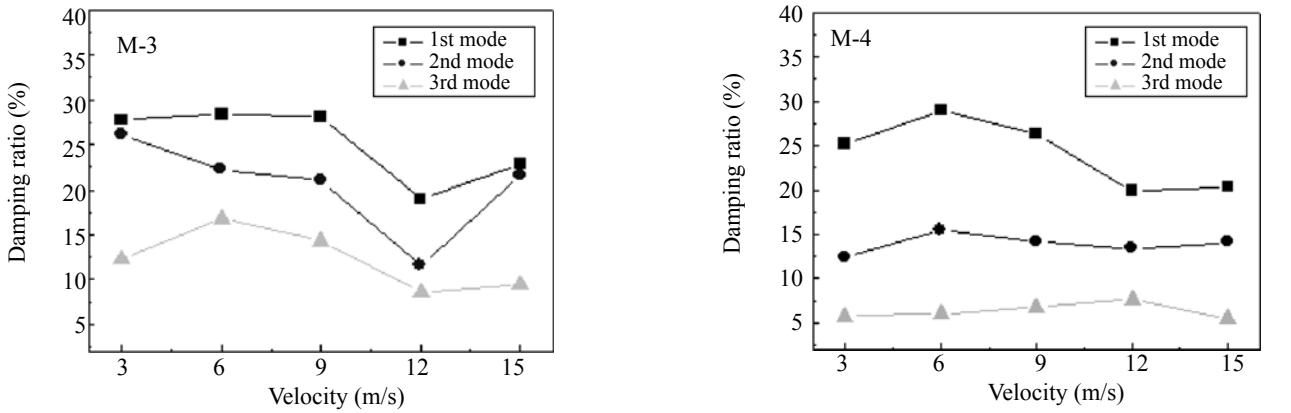

(c) 90º angle of attack

Fig. 17 Damping ratio for different wind speeds and angles of attack

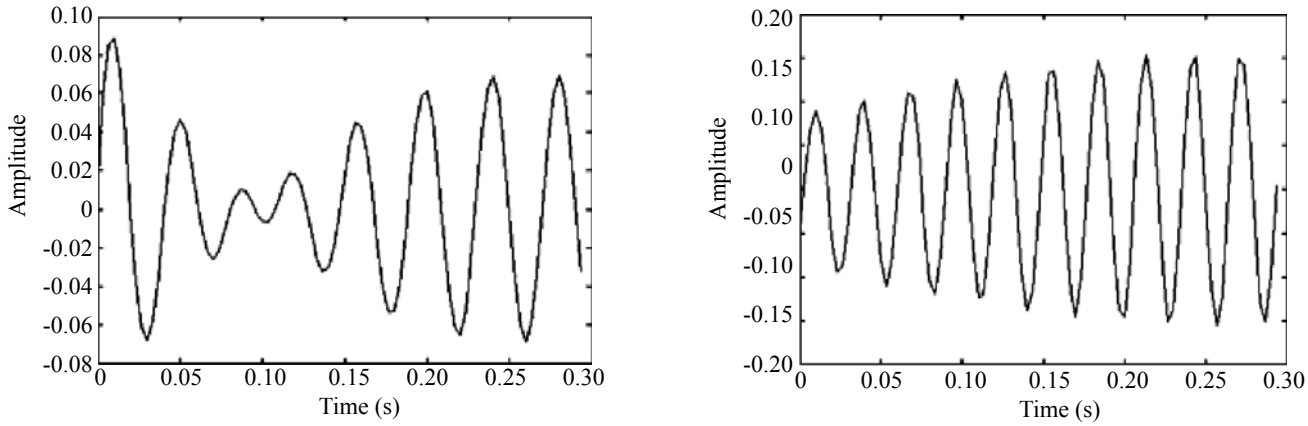

Fig. 18 Signals corresponding to negative aerodynamic damping

(2) The influence of the added mass is not as strong when compared to the aerodynamic damping, and the influence becomes even weaker as the wind speed increases.

(3) The negative aerodynamic damping is obtained for some areas in some cases, while global unstable vibration was not observed.

Note that the results presented in this paper are preliminary, as wind-structure interaction is very complicated and the number of models tested is not large enough to provide absolute conclusions. These results should be further investigated by more tests, and studied theoretically and numerically to better explain and understand the mechanism behind the behaviors.

Acknowledgement

The authors appreciate the discussions with and suggestions from Dr. Xinzhong Chen, Department of Civil and Environmental Engineering, Texas Tech University.

References

Daw DJ and Davenport AG (1989), "Aerodynamic Damping and Stiffness of a Semi-circular Roof in Turbulent Wind," *Journal of Wind Engineering and Industrial Aerodynamics*, **32**: 83–92.

Elashkar I and Novak M (1983), "Wind Tunnel Studies of Cable Roofs," *Journal of Wind Engineering and Industrial Aerodynamics*, **13**: 407–419.

Ibrahim SR (1977), "Random Decrement Technique for Modal Identification of Structures," *Journal of Spacecraft and Rockets*, **14**(11): 696–700.

Il'chenko AV and Temnenko VA (1993), "Oscillations of a Membrane That is Orthogonal to a Flow: Asymptotics of Large Stresses," *Journal of Mathematical Sciences*, **65**(2): 1072–3374.

Ishii K (1997). "Membrane Structures in Japan — Technologies for Supporting Membrane Structures," *IASS International Symposium on Shell & Spatial Structures*, Singapore, pp. 15–26.

Kawai H, Yoshie R, Wei R and Shimura M (1999), "Wind-induced Response of a Large Cantilevered Roof," *Journal of Wind Engineering and Industrial Aerodynamics*, **83**: 263–275.

Kawamura S and Kiuchi T (1986). "An Experimental Study of a One-membrane Type Pneumatic Structure – Wind Load and Response," *Journal of Wind Engineering and Industrial Aerodynamics*, **23**: 127–140.

Novak M and Kassem M (1990), "Free Vibration of Light Roofs Backed by Cavities," *Journal of the Engineering Mechanics Division*, **116**(3): 549–564.

Ohkuma T and Marukawa H (1989), "Vibration-induced Wind Pressure on Large Span Flat Roof and Its Application," *Proceedings of the 2nd Asia-Pacific Symposium on Wind Engineering*, Beijing, China, pp. 26–29.

Qin J (2008), "Dynamic Characteristics of Tensioned Cable-membrane Structures," *Spatial Structures*, **14**(2): 42–47. (in Chinese)

Seybert AF (1981), **"**Estimation of Damping from Response Spectra," *Journal of Sound and Vibration*, **75**(2): 199–206.

Takeda T, Kageyama M and Homma Y (1986), "Experimental Studies on Structural Characteristics of a Cable-reinforced Air-supported Structure. Shells," *Membrane and Space Frames, Proceedings of IASS Symposium*, Osaka, pp. 141–148.

Wang J and Yang Q (2003), "Calculation on Added Mass of Structures in Fluid Environments," *Journal of Beijing Jiaotong University*, **27**(1): 40–43. (in Chinese)

Wang J, Yang Q, Wu Y and Zhang L (2003), "Methods for Calculating Added Mass of Fabric Structures," *Spatial Structures*, **9**(3): 38–41. (in Chinese)

Wu Y, Yang Q and Shen S (2008), "Wind Tunnel Tests on Aeroelastic Effect of Wind-induced Vibration of Tension Structures," *Engineering Mechanics*, **25**(1): 8–15. (in Chinese)

Yang Q and Liu R (2005), "On Aerodynamic Stability of Membrane Structures," *International Journal of Space Structures*, **20**(3): 181–188.

Yang Q, Wang J and Wang L (2003), "Interaction of Wind with Fabric Structures," *Spatial Structures*, **9**(1): 20–24. (in Chinese)

Yang Q, Wu Y and Zhu W (2008), "Experimental Study on the Static Interaction Between Membrane Structures and Air", *China Civil Engineering Journal*, **41**(5): 19–25. (in Chinese)